Self-Powered Ultraviolet Photodetectors Driven by Built-In Electric Field

Longxing Su, Wei Yang, Jian Cai, Hongyu Chen, and Xiaosheng Fang*

Self-powered ultraviolet (UV) photodetectors, which have vast applications in the military and for civilian purposes, have become particularly attractive in recent years due to their advantages of high sensitivity, ultrasmall size, and low power consumption. In particular, self-powered UV photodetectors driven by a built-in electric field cannot only detect UV signals but also be powered by the incident signals instead of external power. In this concept, the key issues and most recent developments on photovoltaic type UV photodetectors driven by p–n homojunction, heterojunction, and Schottky junction are surveyed. This should generate extensive interest in this field and encourage more researchers to engage in and tackle the scientific challenges.

1. Introduction

As an important component of electromagnetic radiations, ultraviolet (UV) radiation (10–400 nm)[1] is one of the strongest radiations in natural world, and it has a profound influence on organic life and inorganic existence.[2–4] Typically, UV radiation is mainly divided into two classes: (1) electromagnetic radiation coming from natural environment, namely solar radiation (**Figure 1**a);[5] (2) artificial UV rays produced by low/high-pressure mercury lamp, UV light emitting diode (LED), gas welding arc, etc. Plank's black body theory identifies that objects with temperature of over 1200 °C can obviously emit UV light and the proportion of higher energy UV radiation band increases as temperature goes up.[6] According to the standard of International Commission on Illumination, UV radiation is divided into three bands (Figure 1b): UVA: 320–400 nm, UVB: 280–320 nm, and UVC: 10–280 nm.[1] Additionally, UV radiation with wavelength from 220 to 280 nm, also called solar blind UV radiation, does not exist on the surface of the earth, and UV radiation with wavelength below 180 nm is called vacuum UV radiation. UV radiation has a strong influence in the survival and development of humankind. For instance, 90% of

Dr. L. X. Su, W. Yang, J. Cai, Prof. X. S. Fang
Department of Materials Science
Fudan University
Shanghai 200433, P. R. China
E-mail: xshfang@fudan.edu.cn
Dr. H. Y. Chen
Department of Physics
Harbin Institute of Technology
Harbin 150001, P. R. China

The ORCID identification number(s) for the author(s) of this article can be found under https://doi.org/10.1002/smll.201701687.

the Vitamin D needed by human body, which contributes to robust bone growth, is originated from the interaction between UVB radiation and human's stratum corneum.[7] Nevertheless, excessive dose of UVB radiation can accelerate the aging of human skin and even result in skin cancer. Therefore, the development of UV photodetectors with applications in environmental monitoring, flame detection, geology detection, space communication, chemical, and pharmaceutical analyses is desperately in demand.[8] Here, Figure 1c summarizes the current and possible future applications of UV photodetectors.

In the last two decades, world economic development had been driven by information technology (IT).[9] Twenty years ago, Internet technology which marks with the widespread use of personal computer (PC) had a significant impact on modern society. Subsequently, the fourth generation (4G) mobile Internet technology which emerged around ten years ago further strengthened the interactions of humankind and boomed the development of commercial economy. Looking toward world technology trends over the next ten years, intelligent hardware based on sensor networks is a remarkable field that may drive the world development. In near future, "Internet of things" which will integrate sensors and objects with network will become a hot research area, and versatile sensors will be distributed and widely used in every corner of the world. For example, conventional forest fire prevention method, which depends on patrol aircrafts and sparsely located fire control stations, is uneconomic and very inefficient. In contrast, densely located high-performance UV photodetectors linked with GPS systems can be used as a more efficient fire monitor. Hence, it is highly expected that future sensors may exhibit supersensitivity, high response speed, extremely low power consumption, ultrasmall size, and extraordinary multifunctionality.[10,11]
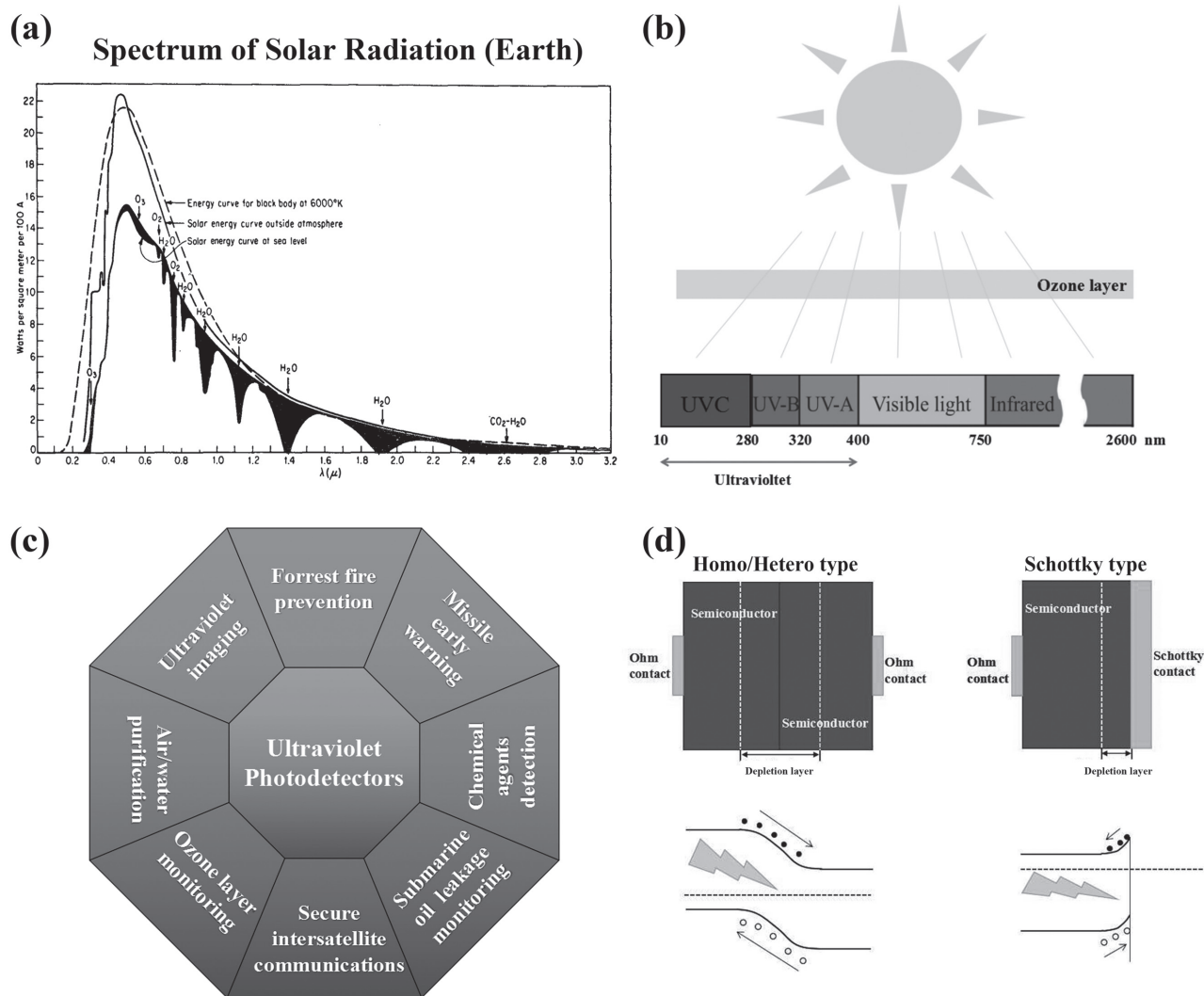
Conventional UV photodetector need to be driven by external power source, typically it is battery. However, such power supplies are not ideal for a future smart sensor system: (1) the materials used for batteries are likely to be potentially hazardous to human's health and environmental unfriendly, extra cost and processes such as battery recycling have to be considered if commercial batteries were used as the power source; (2) the numbers of UV photodetectors involved in the network will be tremendous, so replacing such individual battery in each circuit would be an arduous task. Therefore, sustainable, independent, and maintenance-free UV photodetectors which can harvest energy from the environment are highly desired in

Figure 1. a) Solar irradiation spectrum with and without atmospheric absorption;[5] b) waveband classification of solar radiation and ultraviolet region; c) current and future applications of UV photodetectors; d) schematic diagrams of working principles based on self-powered homo/heterojunction and Schottky junction UV photodetectors. a) Reproduced with permission.[5] Copyright 1974, American Meteorological Society.

such areas as forest fires prevention and submarine oil leakage monitoring.

By now, there have been numerous reports on self-powered UV photodetectors. Those self-powered UV photodetectors can be divided into two groups according to the ways of energy conversion:[8] one type contains photoconductive devices integrated with energy harvesting unit, which can harvest the mechanical energy or chemical energy; the other type is developed by exploiting photovoltaic effect (built-in electric field) through p–n homojunction, heterojunction, or Schottky junction. Compared with the photovoltaic type devices, photoconductive devices usually have better figure of merits (e.g., responsivity and photocurrent) due to the external bias.[12–14] In order to harvest the vibration-based mechanical energy, four techniques including electromagnetic induction,[15] MEMS-based electrostatic energy harvester,[16] magnetostrictive actuator,[17] and piezoelectric resonator[18,19] are developed. These energy harvesting units need to be equipped with an extra energy storage

module (e.g., capacitor). For photo-electrochemical-type UV photodetectors,[20] devices may stop working when the chemical reactants run out. In contrast, UV photodetectors driven by built-in electric field (photovoltaic type) can not only detect the UV signals but also be powered by these incident signals. In photovoltaic-type UV photodetector (as schematic shown in Figure 1d), space charge region (or depletion layer) is formed near the homo-interface, hetero-interface, and semiconductor/metal-interface due to the spontaneous diffusion of free carriers. Subsequently, built-in electric field, which is necessary for the separation of photogenerated e–h pairs, is generated in the junction area. When UV light irradiate on the photodetector, photogenerated e–h pairs in this area can be effectively separated and then photocurrent generates.

So far, there have been numerous progresses in photovoltaic-type self-powered UV photodetectors. It is still extremely important to understand the physical mechanism of these devices in order to develop high-performance self-powered UV

ADVANCED
SCIENCE NEWS
www.advancedsciencenews.com

NANO MICRO
small
www.small-journal.com

Table 1. UV photodetector parameters.[1,18]

Quantity	Symbol	Unit	Definition
Responsivity	R	A·W^{-1}	Photocurrent flowing in the detector divided by incident optical power.
Response time	t_r, t_d	s	Rise time (t_r) and decay time (t_d) are defined as the time in which photocurrent increase from 10% to 90% and drop from 90% to 10% of its maximum value.
Dark current	I_d	A	Current flowing in the absence of illumination. Under zero bias, this value is equal to zero at steady state.
Quantum efficiency	η	%	The ratio of photocurrent to photon fluence incident on the device.
Noise current	I_{noise}	A·Hz$^{-1/2}$	The random root mean square fluctuation in current as the bandwidth is limited to 1 Hz.
Noise-equivalent power	NEP	W·Hz$^{-1/2}$	The optical signal in watts at which the electrical signal-to-noise ratio in the detector is unity (0 dB), and the bandwidth is limited to 1 Hz. This value determines the minimum detectable power.
Normalized detectivity	D^*	cm·Hz$^{-1/2}$·W^{-1} (Jones)	A measure of detector sensitivity that enables comparison even when bandwidth B and detector area A are different. $D^* = (A \cdot B)^{-1/2}/\text{NEP}$.

photodetectors. In this paper, a selection of the frontier works in this area is reviewed. Firstly, various parameters (responsivity, quantum efficiency, response time, and so forth) that evaluate the performance of a self-powered UV photodetector are briefly introduced. Then, we will focus on the discussions of recent efforts and significant progresses in this field. After that, the possible challenges and opportunities for these techniques are proposed.

2. UV Photodetector Parameters

Table 1 summarizes the main parameters used to evaluate the performance of UV photodetectors.[1,21] Responsivity R is a physical quantity representing the photoelectric conversion ability of a UV photodetector. It is determined by the quantum efficiency η (numbers of electron–hole (e–h) pairs generated per incident photon) and gain g (numbers of carriers detected per photongenerated e–h pair) of the photodetector, using the following equation:[1]

$$R = \frac{\lambda \eta}{hc} qg \tag{1}$$

Where λ is the radiation wavelength, h is Planck constant, c is the speed of light, and q is the electron charge. Typically, unless under the condition of avalanche, the quantum efficiency η of a photovoltaic photodetector cannot be higher than 100% and the gain g is equal to one. Response time describes the signals tracking ability of a UV photodetector. Under several particular circumstances, such as aerial battle and missile defense, operators, whose brain reaction speed is typically longer than 0.2 s,[22] need to make a decision immediately according to the detected signals. Hence, a UV photodetector with rapid response is extremely significant.

Noise currents I_{noise} including shot noise, thermal noise, and low-frequency noise represent the weak signal detection capability of UV photodetectors. In general, low-frequency noise becomes dominant when the device works under low frequency. Nevertheless, thermal noise dominates as the device working under high frequency. As for comparing the sensitivities of

UV photodetectors, signal-to-noise level at a given illumination intensity is provided. Alternatively, one can examine the noise-equivalent power (NEP), which is the optical power at which the signal-to-noise ratio is 1 (or 0 dB). Unless the noise level is ultralow, single-photon detection is impossible.[21] The detectivity D^* seeks to normalize the variations in speed of response and devices area, thus providing a parameter that enables the comparison among different devices. This parameter reflects the ability to detect the weak signal from the noise environment and should be improved as high as possible.

3. Self-Powered UV Photodetectors Driven by Built-In Electric Field

In self-powered UV photodetectors based on photovoltaic effect, photoinduced e–h pairs are directionally separated by the built-in electric field from p–n homojunction, heterojunction, or Schottky junction, thus generating output photocurrent. Generally, photovoltaic-type UV photodetectors exhibit much lower dark current and higher sensitivity than that of photoconductive ones. What's more, a strong built-in electric field and a depletion layer can be formed near the junction region, thus contributing to effective charges separation and resulting in rapid response.

3.1. Self-Powered UV Photodetectors Based on p–n Homojunction

In a self-powered p–n homojunction-type UV photodetector, built-in electric field with direction from n-layer to p-layer is generated near the homo-interface due to the spontaneous interdiffusion of free electrons from n-side and free holes from p-side. Homojunction-type self-powered UV photodetectors usually exhibit great potentials in extreme working conditions due to their great resistance to both chemical etch and thermal deterioration, since many structural defects near the p–n interface can be avoided owing to their perfect lattice match. In addition, these energy band matching p–n homojunction devices with single bandgap usually have mono-cutoff wavelength.

**ADVANCED
SCIENCE NEWS**

www.advancedsciencenews.com

NANO · MICRO

small

www.small-journal.com
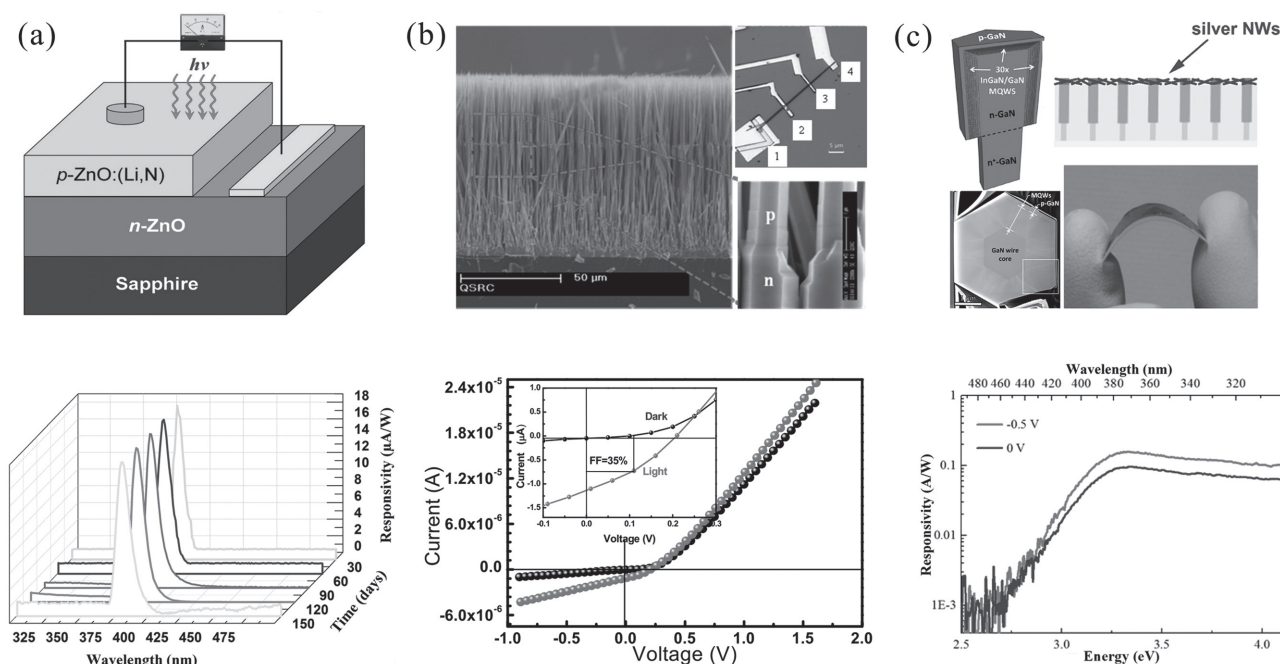
Figure 2. a) Self-powered UV photodetector based on *p*-ZnO:(Li,N)/*n*-ZnO homojunction, Copyright 2013, American Institute of Physics; b) Self-powered UV photodetector based on a coaxial single ZnO nanowire *p–n* homojunction, Copyright 2012, Institute of Physics; c) Flexible self-powered UV photodetector based on nitride core–shell *p–n* homojunction nanowire. Copyright 2016, American Chemical Society.

Recently, homojunction UV photodetectors based on wide bandgap semiconductors such as nitride and oxide materials have been reported. Among them, ZnO[23] and GaN[24] have drawn extensive attentions for their high conductivity, excellent stability, and mature preparation process, which are of great importance for the widespread applications of high-performance self-powered UV photodetectors.

The *p*-ZnO:(Li,N)/*n*-ZnO homojunction device shown in **Figure 2**a is a typical self-powered UV photodetector that is fit for large-scale fabrication.[25] Identical *p–n* junction with strong built-in electric field results in rapid charge separation and fast response. This self-powered device shows selective response to a very narrow spectrum range. According to its photoresponse spectrum under zero bias, a dominant peak at around 380 nm with a full width at half maximum of only 9 nm is found. Here, the highly spectrum-selective characteristic is ascribed to the neutral region in ZnO:(Li,N) layer which serves as an optical filter. Furthermore, due to the perfect crystal quality and homojunction interface prepared by molecular beam epitaxy (MBE) technique, this photodetector exhibits an excellent stability in performance.

Compared to 2D films, 1D materials with large surface-to-volume ratio show higher responsivity because more light can be absorbed by light trapping[26] or antireflection effects.[27] Thanks to the nanostructures, 1D arrays can stand severe deformation without damage, thus they are also suitable for flexible devices. Additionally, 1D material-based flexible devices can be fabricated by directly growth on conductive plastic substrate,[28] a two-step transfer-assembly process after mechanical peeling[29] or under-etching.[30] Both 1D core–shell and coaxial *p–n* structures can be utilized to fabricate self-powered UV photodetectors. As shown in Figure 2b, a single

coaxial ZnO nanowire diode consists of as grown *n*-type segment and Arsenic doping *p*-type segment is successfully synthesized and act as a good photovoltaic UV photodetector.[31] Due to the limited junction area for light absorption, the device shows poor sensitivity and responsivity under zero bias. However, compared with coaxial *p–n* structure, core–shell structure can exhibit higher self-powered potential due to its wider active area for light absorption. As shown in Figure 2c, a novel flexible UV photodetector based on core–shell *p–n* homojunction GaN nanowires (NWs) embedding in a polymer layer is prepared after well-controlled metal organic vapor phase epitaxy (MOVPE) growth on sapphire substrate.[32] Transparent silver nanowire networks and Ni/Au metallic layer serve as the positive and negative electrodes, respectively. InGaN/GaN quantum wells between *p*-layer and *n*-layer are designed to attenuate the nonuniform electric field caused by the piezoelectric effect, which may increase the Auger-processes[33] and reduce the quantum efficiency. In this way, the photodetector shows a peak responsivity of 96 mA W^{-1} at 370 nm and rapid response speed (−3 dB cutoff at 35 Hz) under zero bias. In addition, this polymer membrane embedding core–shell nanowire photodetector ensures high mechanical flexibility, which is extremely propitious to the development of next generation portable and wearable electronics.

Although considerable progresses on self-powered *p–n* homojunction UV photodetectors have been realized, limitations still exist against its large-scale applications. Firstly, exploiting low-cost fabrication methods for high-quality active materials is still unsolved. To date, excellent performance devices are usually prepared by using high-cost techniques like MBE and MOVPE. Even though homojunction nanostructures based on ZnO, SnO$_2$, TiO$_2$, etc. have been successfully

ADVANCED
SCIENCE NEWS
www.advancedsciencenews.com

NANO MICRO
small
www.small-journal.com

prepared through low-cost method like solution process.[34–37] Nevertheless, few of them can work without external power sources. In terms of devices' performances and scale-up possibility, vapor-phase-based methods like MBE and MOCVD have more advantages than wet-chemical-based method like sol-gel as the materials fabricated by the former have much higher crystal quality and better controllability. However, considering the factor of fabrication cost, wet-chemical-based method is much better due to its uncomplicated preparation process and inexpensive preparation equipment. Secondly, effective doping is still a severe restriction for many wide bandgap semiconductors. Low dopant solubility, obvious compensation by native defects, deep impurity level,[38] and structural bistability known as AX and DX centers[39] strongly bring difficulties to effective p-type doping in wide bandgap oxides and nitrides. Therefore, intrinsic low conductivity, especially the low hole mobility of current wide bandgap semiconductors severely restricted their further applications of self-powered UV photodetectors.

3.2. Self-Powered UV Photodetectors Based on Heterojunction

Similar to self-powered UV photodetectors based on p–n homojunction, heterojunction self-powered UV photodetector can also operate without external power sources. Inner potential difference, which is necessary for the separation of photogenerated e–h pairs, can be automatically created due to the Fermi energy difference between two different dissimilar semiconductors. Subsequently, inner electrical field induced by the potential difference will guide the movement of photogenerated

carriers and give rise to photocurrent. Magically, numerous wide bandgap semiconductors, such as ZnO, GaN, ZnSe, and ZnTe, exhibit unipolar conductive property.[40] That is to say that these wide bandgap semiconductors can facilely and easily realize n-type (p-type) through doping or controlling intrinsic defect concentrations. Nevertheless, their counterparts are rather difficult to achieve. Hence, compared with p–n homojunction UV photodetector, heterojunction UV photodetectors offer more choices and possibilities by matching various inorganic and organic p-type (n-type) semiconductors, enabling multifunctional, flexible, foldable, and biocompatible devices.

In fact, numerous inorganic/inorganic and inorganic/organic self-powered UV photodetectors based on heterojunction, such as p-NiO/n-ZnO,[41] p-CuSCN/n-ZnO,[42] p-GaN/n-ZnO,[43,44] n-R/A TiO$_2$,[45] n-Ga$_2$O$_3$/n-ZnO,[46] p-NiO/n-TiO$_2$,[47] p-polyaniline (PANI)/n-TiO$_2$,[48] p-PANI/n-MgZnO,[49] and so forth,[50–52] have already been reported by many groups. Su and coworkers fabricated a heterojunction UV photodetector based on high crystal quality p-GaN/n-ZnO bilayers which were epitaxially grown on c-sapphire substrate (shown in **Figure 3**a).[43] The photodetector exhibits obvious photoresponse, and the peak responsivity is 0.68 mA W^{-1} at 358 nm under zero bias, which is one of the best values reported on p-GaN/n-ZnO heterojunction photodetectors. The high performance of the photodetector can be mainly ascribed to the advanced thin film growing techniques and the excellent lattice match between GaN (wurtzite, a = 0.318 nm, c = 0.518 nm) and ZnO (wurtzite, a = 0.325 nm, c = 0.523 nm). The most prominent advantages of their work are the thin film preparation method and device fabrication process, which are compatible with the commercialized
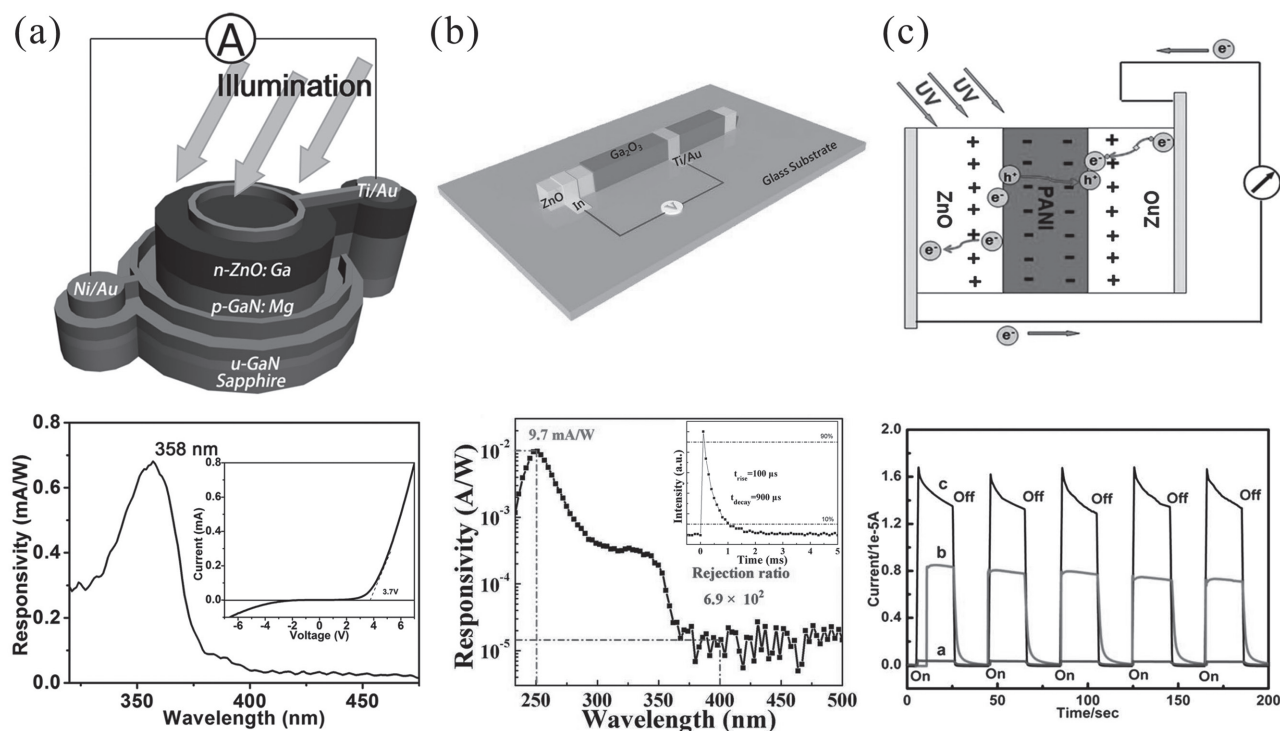
Figure 3. a) Self-powered UV photodetector based on p-GaN/n-ZnO heterostructure. Copyright 2014, American Institute of Physics. b) Ultrahigh performance self-powered solar blind photodetector based on ZnO–Ga$_2$O$_3$ heterostructure. Copyright 2017, Wiley-VCH. c) A sandwich-structured self-powered UV photodetector based on n-ZnO/p-PANI/n-ZnO. Copyright 2012, Royal Society of Chemistry.

**ADVANCED
SCIENCE NEWS**
www.advancedsciencenews.com

NANO · MICRO

small
www.small-journal.com

detector production process that has been successfully proved by the market. Besides $p–n$ heterojunction, $n-n$ heterojunction is another choice that can also generate built-in electric field due to the Fermi energy difference between two materials. As shown in Figure 3b, Zhao and coworkers reported an ultrahigh responsivity self-powered solar blind photodetector based on n-ZnO/n-Ga$_2$O$_3$ core–shell heterostructures.[46] A simple one-step vapor–solid progress method was used to synthesize highly crystallized ZnO–Ga$_2$O$_3$ heterostructure core–shell microwires. These ZnO–Ga$_2$O$_3$ microwires are quite different from previous reported samples prepared by two-step chemical vapor deposition method, in which many defects exist in the grain boundaries.[53] Under zero bias, the self-powered solar blind photodetector shows a high UV–vis rejection ratio of 6.9×10^2 and an ultrahigh responsivity (9.7 mA W^{-1}) at 251 nm. As a result of conduction band offset between ZnO and Ga$_2$O$_3$, the very high resistance of Ga$_2$O$_3$ ($\approx$TΩ) and relative low resistance of ZnO ($\approx$kΩ), depletion layer mainly locates at Ga$_2$O$_3$ side and response signal from ZnO is rather weak. The response from ZnO can be further eliminated by operating at reverse bias. The device also has a fast response speed with the rise time $\approx$100 µs and decay time of $\approx$900 µs, which are much shorter than that of photoconductive-type Ga$_2$O$_3$ solar blind photodetectors ($\approx$seconds). Under the on/off radiation of 254 nm UV light (1.67 mW cm^{-2}), the dynamic response of the photodetector exhibits excellent reproducibility and stability without external power sources. This kind of low-dimensional heterojunction design technique would provide a novel approach to realize high-performance flexible self-powered UV photodetectors.

Due to the facile synthesis method, low cost, and high flexibility of organic conductive polymers, several efforts were made to develop composite structure of organic semiconductor polymers and inorganic semiconductors.[54] However, the photoelectric conversion efficiency and the photocurrent are still very low due to the high defect concentration and low carrier mobility in organic materials. This implies that a simple junction could not completely replace the external bias voltage to control the movement of photogenerated electrons and holes. In this case, a self-powered sandwich-structured UV photodetector composed of two n-type ZnO nanorods layers and one p-type PANI NWs layer has been proposed (Figure 3c).[54] ZnO nanorods were grown on indium tin oxide glass electrode through a hydrothermal process. Two ZnO nanorod array layers were separated by a thin layer of PANI NWs synthesized by the liquid–liquid interface method.[55] In this device structure, two opposite directional inner electric fields were formed in the interfaces of ZnO/PANI/ZnO. With further modification of the polystyrene sulfate, the transition probability of electrons from valence band to conduction band in ZnO nanorod is significantly enhanced, which restrains the recombination of $e–h$ pairs. Subsequently, high photocurrent ($\approx$1.4 $\times$ 10^{-5} A) and photosensitivity ($\approx$1.68 $\times$ 10^5) have been achieved under zero bias.

Even though heterojunction-type self-powered UV photodetectors give rise to so many advantages mentioned above and have already achieved several significant progresses. Many challenges, such as interface defects caused by different crystal structure and lattice mismatch between hetero-materials, low mobility of organic semiconductor and complicated preparation process, must be considered when choosing candidate materials for composite structures. In the future, to further improve the performance of the heterojunction-type self-powered photodetectors, crystal structure, lattice match, carriers' transport abilities, and life time between different semiconductors should be taken into consideration. Furthermore, two different semiconductors should be chosen to meet the requirement of forming type-II heterojunction (i.e., staggered gap).

3.3. Self-Powered UV Photodetectors Based on Schottky Junction

Apart from self-powered UV photodetectors based on $p–n$ homojunction and heterojunction, UV photodetectors based on Schottky junction can also operate without external power sources owing to the photovoltaic effect.[56] Furthermore, with the advantages of low-cost fabrication, Schottky-type photodetectors with ultrarapid response and high photosensitivity are more preferable in future applications.[57] Generally, built-in electric field, which separates the photogenerated $e–h$ pairs and gives rise to circuit current, is formed due to the electrons spontaneously diffusion caused by work function difference between contact metal and semiconductor. Unfortunately, the surface state of semiconductor could seriously affect the diffusion process. Therefore, in order to achieve high performance, quantities of endeavors are required to optimize the stability and quality of Schottky contact. Up to present, several investigations of self-powered Schottky-type UV photodetectors made from different semiconductors have been reported.[58–62]

As shown in **Figure 4**a, a novel type of self-powered Schottky-type ZnO photodetector based on asymmetric meta-semiconductor-metal (MSM) structure was fabricated.[63] Herein, different widths of depletion region are formed near the wide finger and narrow finger Au electrodes. As the asymmetric ratio (the width of wide finger/the width of narrow finger) is enhanced to 20:1, the device shows extremely high performance with responsivity of 20 mA W^{-1} and response speed of 4 µs under zero bias. The typical photovoltaic characteristic in the asymmetric MSM photodetector is ascribed to the different electric potential distributions near the wide finger and narrow finger. Their finding provides a new route to realize self-powered UV photodetectors by using just one kind of contact metal through a one-step evaporation process. Recently, some researchers further boost the photovoltaic effect through piezoelectric effect.[64,65] Lu and coworkers improved the performance of ZnO NWs/Au Schottky-type self-powered UV photodetector by modulating the piezoelectric polarization induced by artificial strains.[66] As shown in Figure 4b, the output current increases obviously as the tensile strain gradually increases, which could be introduced and calculated by applying different curvatures on the flexible polystyrene substrate. Interestingly, both sensitivity and photocurrent increase linearly with increased tensile stain. Increase of 440% in photocurrent along with an over 5 times enhancement in sensitivity is obtained when a 0.58% tensile strain on the device is induced. This improvement originates from the monotonical relation of Schottky barrier height with the tensile strain. It could be fairly verified that the stronger and wider built-in electric field could

ADVANCED
SCIENCE NEWS
www.advancedsciencenews.com

NANO · MICRO
small
www.small-journal.com
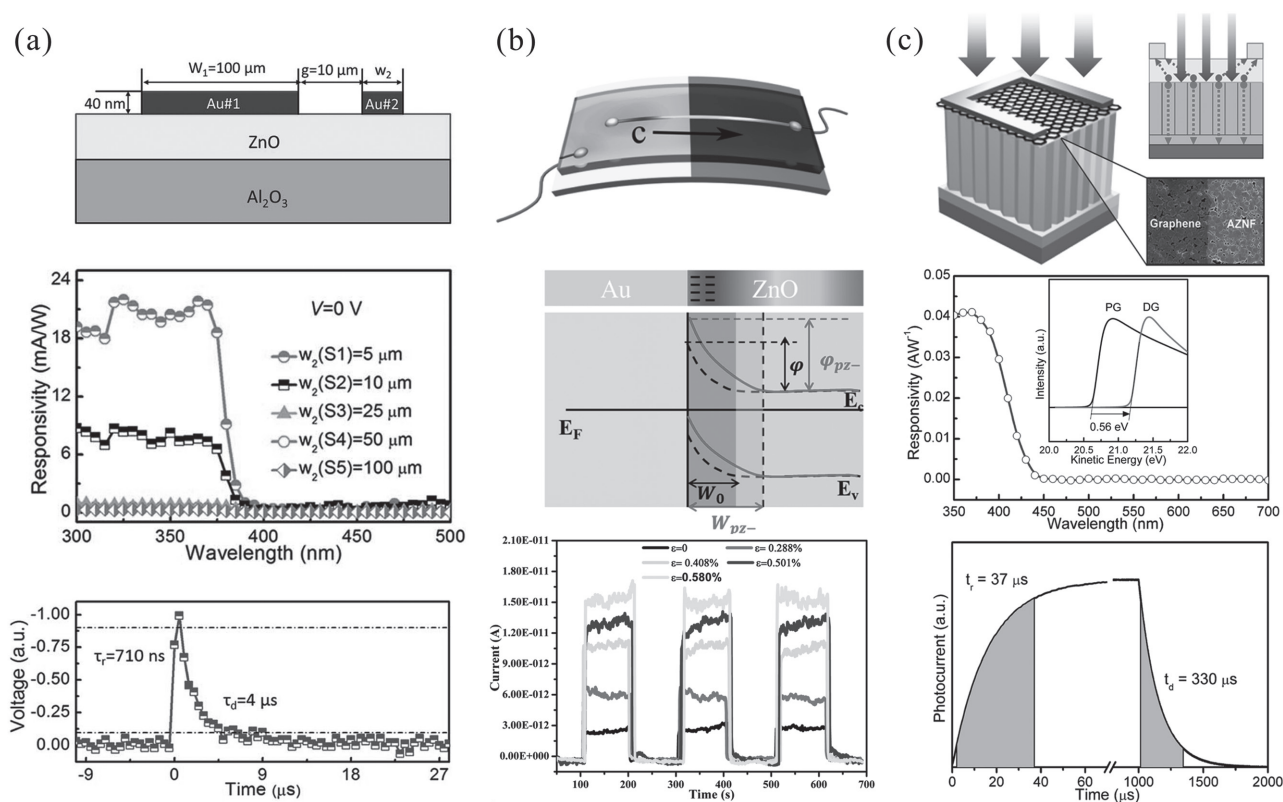
Figure 4. a) A self-powered ZnO MSM UV photodetector using an asymmetric pair of Au electrodes. Copyright 2014, Royal Society of Chemistry. b) Flexible self-powered UV photodetector based on ZnO/Au Schottky junction. Copyright 2014, American Chemical Society. c) A self-powered fast response UV photodetector based on graphene/ZnO:Al nanorod arrays film. Copyright 2017, American Chemical society.

effectively promote the separation and extraction of the photo-generated e–h pairs. Their study extends the performances and flexibility of optoelectronic devices constructed by piezoelectric materials.

With regards to the trend of next generation self-powered UV photodetector, large-scale deposition of conventional contact metals goes against the flexibility and wearability of the devices. In addition, these metal contacts still limit the further improvement of Schottky barrier due to their high cost and incident light absorption. Thus, some other conductive materials are introduced to replace the contact metals. They not only diversify the Schottky contact family but also promote the device performance and show potential on flexible devices. Among them, graphene exhibits great potential due to its high transparent conductivity and excellent mechanical properties.[10] Duan and coworkers prepared a self-powered Schottky UV photodetector based on graphene/ZnO:Al nanorod-array-film (AZNF) (Figure 4c).[67] Different from other previous efforts, this photodetector has a very stable Schottky barrier which does not disappear even under UV light radiation. The significant improvement in stability of graphene/semiconductor barrier can be ascribed to two reasons: a two-step surface treatment process and Au^{3+} doping into graphene. After Au^{3+} doping, the work function of graphene has been enhanced to 0.56 eV, which gives rise to a remarkable Schottky barrier height. Additionally, interface states between graphene and AZNF are distinctly reduced after the two-step surface

treatment. In this way, the self-powered photodetector exhibits a UV–vis ratio of ≈10^2, a responsivity of 39 mA W^{-1}, a rise time of 37 µs and a decay time of 330 µs. Under extremely low-radiation condition, the responsivity of the device still remains at a satisfying value.

Besides great advantages and progresses mentioned above, there are still several drawbacks on Schottky-type UV photodetector. Firstly, the depth of depletion layer in Schottky junction is relatively shallow. This will restrict the effective separation of e–h pairs. Secondly, Schottky barrier is serious affected by the surface state of semiconductor, which requires precisely control of the interface between metal and semiconductor. Therefore, efforts and attentions need to be paid to strengthen the barrier height and the stability of the Schottky junction.

4. Conclusion and Outlook

In this concept, we focus on the self-powered UV photodetectors driven by built-in electric field, which is extremely important for the applications in UV detection. Recent progresses and challenges in this field (devices based on p–n homojunctiom, heterojunction, and Schottky junction) are systematically discussed. Systematic comparison of photodetector performances based on these devices has been summarized in **Table 2**. Additionally, the developing tendency of next generation photovoltaic-type UV is also proposed. It is clear that these self-powered devices

**ADVANCED
SCIENCE NEWS**

www.advancedsciencenews.com

NANO · MICRO

small

www.small-journal.com

Table 2. Comparison of the photodetector performances for self-powered UV photodetector driven by built-in electric field.

Photodetector	Wavelength of Detection	Responsivity	Sensitivity at 0 V	Rise time	Decay time	Detectivity [Jones]	Reference
p-ZnO:(Li,N)/*n*-ZnO		≈18 μA W^{-1}	–	–	–	–	[25]
p-ZnO:(As)/*n*-ZnO	≈370 nm	–	≈10^6	30 ms	50 ms	–	[31]
p-GaN/*n*-GaN Core–shell	370 nm	96 mA W^{-1}	≈10^3	<0.1 s	<0.1 s	–	[32]
p-CuSCN/*n*-ZnO	370 nm	20 mA W^{-1}	–	–	–	–	[42]
p-GaN/*n*-ZnO	358 nm	0.68 mA W^{-1}	–	–	–	–	[43]
n-R/A TiO$_2$	365 nm	–	–	−0.3 s	−0.2 s	–	[45]
n-Ga$_2$O$_3$/*n*-ZnO	251 nm	9.7 mA W^{-1}	≈5 × 10^3	100 μs	900 μs	6.29 × 10^{12}	[46]
p-NiO/*n*-TiO$_2$	350 nm	≈65 μA W^{-1}	≈14	1.2 s	7.1 s	1.1 × 10^9	[47]
p-PANI/*n*-TiO$_2$	320 nm	3.6 mA W^{-1}	1.3 × 10^3	3.8 ms	30.7 ms	3.9 × 10^{11}	[48]
p-PANI/*n*-MgZnO	250 nm	160 μA W^{-1}	≈10^4	<0.3 s	<0.3 s	1.5 × 10^{11}	[49]
n-ZnO/*p*-PANI/*n*-ZnO	365 nm	–	1.68 × 10^5	–	–	–	[54]
Pt-GaN-Ni	UV	30 mA W^{-1}	4.67 × 10^5	<0.1 s	<0.1 s	1.78 × 10^{12}	[61]
ZnO MSM	365 nm	20 mA W^{-1}	–	71 0 ns	4 μs	–	[63]
Ag–ZnO–Au	325 nm	–	≈10^3	0.1 s	0.1 s	–	[66]
Graphene/ZnO	380 nm	≈20 mA W^{-1}	–	37 μs	330 μs	–	[67]

will play a significant role in environmental monitoring, medical analysis, defense technology, and fire protection due to their low power consumption and maintain-free property.

Up to now, numerous efforts have been paid in this field. Despite of the rapid progress that has been made, self-powered UV photodetectors with higher performances are still highly desired for further advanced applications. Therefore, considerable future studies are proposed to fabricate high-performance self-powered UV photodetectors. Firstly, to meet the great demand in weak signal detection, rapider and higher sensitive devices are required. Here, surface plasmon resonance technique would provide a new and robust path toward that purpose. Due to the resonance light absorption caused by surface plasmons, more photogenerated carriers are produced in the active layer and thus contributing to higher photocurrent. In addition, the enhanced electromagnetic field surrounding the plasmonic nanostructure can also accelerate the separation of *e–h* pairs and thus resulting in higher response speed. Secondly, revolutionary concepts are further needed to explore versatile self-powered UV photodetectors toward the intelligent era to break through optical diffraction limit. Innovative techniques should be developed to significantly reduce the size and weight of self-powered UV photodetectors. Thirdly, most of current self-powered UV photodetectors are mainly focused on conventional inorganic semiconductors. In future, some novel and exotic materials, such as *h*-BN, perovskites, and black phosphorus, should be considered. Finally, profit maximization and cost minimization through industrial controlling and mass production are urgently demanded to meet the practical application in marketplace. Nevertheless, most of efforts are mainly focused on the performance and novelty improvement of the UV photodetectors.

In summary, a self-powered UV photodetector driven by built-in electric field can operate independently, sustainably, and wirelessly. As one of the key components of next generation "Internet of things," the development of self-powered UV photodetectors will follow the trend of next generation electronics and move toward multifunctional, portable, super sensitive, ultrasmall, and flexible electronics. This requires the rational synthesis of materials, fabrication of devices, and integration of various devices into a system with multifunctional characteristics and operate without external power sources. Developments in this field will open a new research area and innovate novel techniques.

Conflict of Interest

The authors declare no conflict of interest.

ADVANCED
SCIENCE NEWS
www.advancedsciencenews.com

NANO MICRO
small
www.small-journal.com

[1] E. Monroy, F. Omnès, F. Calle, *Semicond. Sci. Technol.* **2003**, *18*, R33.

[2] B. Diffey, *Phys. Med. Biol.* **1991**, *36*, 299.

[3] S. E. Mancebo, S. Q. Wang, *Rev. Environ. Health* **2014**, *29*, 265.

[4] X. S. Fang, L. F. Hu, K. F. Huo, B. Gao, L. J. Zhao, M. Y. Liao, P. K. Chu, Y. Bando, D. Golberg, *Adv. Funct. Mater.* **2011**, *21*, 3907.

[5] A. Lacis, E. Hansen, *J. Atmos. Sci.* **1974**, *31*, 118.

[6] T. S. Kuhn, *Black-Body Theory and The Quantum Discontinuity, 1894–1912*, University of Chicago Press, Chicago, IL, USA **1987**.

[7] M. F. Holick, *Am. J. Clin. Nutr.* **2004**, *80*, 1678S.

[8] H. Y. Chen, K. W. Liu, L. F. Hu, A. A. Al-Ghamdi, X. S. Fang, *Mater. Today* **2015**, *18*, 493.

[9] Z. L. Wang, *Adv. Mater.* **2012**, *24*, 280.

[10] J. A. Paradiso, T. Starner, *IEEE Pervas. Comput.* **2005**, *4*, 18.

[11] L. Peng, L. Hu, X. S. Fang, *Adv. Funct. Mater.* **2014**, *24*, 2591.

[12] N. Nasiri, R. Bo, F. Wang, L. Fu, A. Tricoli, *Adv. Mater.* **2015**, *27*, 4336.

[13] Q. F. Liu, M. Gong, B. Cook, D. Ewing, M. Casper, A. Stramel, J. Wu, *Adv. Mater. Inter.* **2017**, *4*, 1601064.

[14] R. Bo, N. Nasiri, L. Fu, A. Tricoli, *ACS Appl. Mater. Inter.* **2017**, *9*, 2606.

[15] K. J. Kim, F. Cottone, S. Goyal, J. Punch, *Bell Labs Tech. J.* **2010**, *15*, 7.

[16] S. Meninger, J. O. Mur-Miranda, R. Amirtharajah, A. Chandrakasan, J. H. Lang, *IEEE VLSI Syst.* **2001**, *9*, 64.

[17] L. Wang, F. Yuan, *Smart Mater. Struct.* **2008**, *17*, 045009.

[18] A. Erturk, D. J. Inman, *J. Vib. Acoust.* **2008**, *130*, 041002.

[19] X. Wang, J. Song, J. Liu, Z. L. Wang, *Science* **2007**, *316*, 102.

[20] X. Li, C. Gao, H. Duan, B. Lu, X. Pan, E. Xie, *Nano Energy* **2012**, *1*, 640.

[21] G. Konstantatos, E. H. Sargent, *Nat. Nanotechnol.* **2010**, *5*, 391.

[22] B. Fischer, E. Ramsperger, *Exp. Brain Res.* **1984**, *57*, 191.

[23] K. Liu, M. Sakurai, M. Aono, *Sensors* **2010**, *10*, 8604.

[24] H. Morkoç, A. Di Carlo, R. Cingolani, *Solid-State Electron.* **2002**, *46*, 157.

[25] H. Shen, C. Shan, B. Li, B. Xuan, D. Shen, *Appl. Phys. Lett.* **2013**, *103*, 232112.

[26] E. Garnett, P. Yang, *Nano Lett.* **2010**, *10*, 1082.

[27] P. Yu, C. H. Chang, C. H. Chiu, C. S. Yang, J. C. Yu, H. C. Kuo, S. H. Hsu, Y. C. Chang, *Adv. Mater.* **2009**, *21*, 1618.

[28] H. Zhang, Y. Hu, Z. Wang, Z. Fang, L. M. Peng, *ACS Appl. Mater. Interfaces* **2015**, *8*, 381.

[29] X. Dai, A. Messanvi, H. Zhang, C. Durand, J. Eymery, C. Bougerol, F. H. Julien, M. Tchernycheva, *Nano Lett.* **2015**, *15*, 6958.

[30] C. H. Lee, Y. J. Kim, Y. J. Hong, S. R. Jeon, S. Bae, B. H. Hong, G. C. Yi, *Adv. Mater.* **2011**, *23*, 4614.

[31] H. D. Cho, A. S. Zakirov, S. U. Yuldashev, C. W. Ahn, Y. K. Yeo, T. W. Kang, *Nanotechnology* **2012**, *23*, 115401.

[32] H. Zhang, X. Dai, N. Guan, A. Messanvi, V. Neplokh, V. Piazza, M. Vallo, C. Bougerol, F. H. Julien, A. Babichev, *ACS Appl. Mater. Interfaces* **2016**, *8*, 26198.

[33] Y. Shen, G. Mueller, S. Watanabe, N. Gardner, A. Munkholm, M. Krames, *Appl. Phys. Lett.* **2007**, *91*, 141101.

[34] W. Zheng, X. Li, G. He, X. Yan, R. Zhao, C. Dong, *RSC Adv.* **2014**, *4*, 21340.

[35] T. Yang, X. Qin, H. H. Wang, Q. Jia, R. Yu, B. Wang, J. Wang, K. Ibrahim, X. Jiang, Q. He, *Thin Solid Films* **2010**, *518*, 5542.

[36] W. C. Lee, J. Y. Chen, C. W. Huang, C. H. Chiu, T. Y. Lin, W. W. Wu, *Chem. Mater.* **2015**, *27*, 4216.

[37] C. L. Hsu, Y. D. Gao, Y. S. Chen, T. J. Hsueh, *ACS Appl. Mater. Interfaces* **2014**, *6*, 4277.

[38] C. Park, S. Zhang, S. H. Wei, *Phys. Rev. B* **2002**, *66*, 073202.

[39] G. Hautier, A. Miglio, G. Ceder, G. M. Rignanese, X. Gonze, *Nat. Commun.* **2013**, *4*, 2292.

[40] K. Takahashi, A. Yoshikawa, A. Sandhu, *Wide Bandgap Semiconductors*, Springer, Berlin, Germany **2007**.

[41] P. N. Ni, C. X. Shan, S. P. Wang, X. Y. Liu, D. Z. Shen, *J. Mater. Chem. C* **2013**, *1*, 4445.

[42] J. R. M. Garnier, R. Parize, E. Appert, O. Chaix-Pluchery, A. Kaminski-Cachopo, V. Consonni, *ACS Appl. Mater. Interfaces* **2015**, *7*, 5820.

[43] L. Su, Q. Zhang, T. Wu, M. Chen, Y. Su, Y. Zhu, R. Xiang, X. Gui, Z. Tang, *Appl. Phys. Lett.* **2014**, *105*, 072106.

[44] Y. Q. Bie, Z. M. Liao, H. Z. Zhang, G. R. Li, Y. Ye, Y. B. Zhou, J. Xu, Z. X. Qin, L. Dai, D. P. Yu, *Adv. Mater.* **2011**, *23*, 649.

[45] X. Yu, Z. Zhao, J. Zhang, W. Guo, J. Qiu, D. Li, Z. Li, X. Mou, L. Li, A. Li, *Small* **2016**, *12*, 2759.

[46] B. Zhao, F. Wang, H. Chen, L. Zheng, L. Su, D. Zhao, X. S. Fang, *Adv. Funct. Mater.* **2017**, *27*, 1700264.

[47] L. X. Zheng, F. Teng, Z. Zhang, B. Zhao, X. S. Fang, *J. Mater. Chem. C* **2016**, *4*, 10032.

[48] L. X. Zheng, P. Yu, K. Hu, F. Teng, H. Chen, X. S. Fang, *ACS Appl. Mater. Interfaces* **2016**, *8*, 33924.

[49] H. Y. Chen, P. Yu, Z. Zhang, F. Teng, L. Zheng, K. Hu, X. S. Fang, *Small* **2016**, *12*, 5809.

[50] Y. Y. Lin, C. W. Chen, W. C. Yen, W. F. Su, C. H. Ku, J. J. Wu, *Appl. Phys. Lett.* **2008**, *92*, 205.

[51] Y. Teng, L. X. Song, W. Liu, Z. Y. Xu, Q. S. Wang, M. M. Ruan, *J. Mater. Chem. C* **2016**, *4*, 3113.

[52] Y. Zhang, J. Xu, S. Shi, Y. Gao, C. Wang, X. Zhang, S. Yin, L. Li, *ACS Appl. Mater. Interfaces* **2016**, *8*, 22647.

[53] K. W. Chang, J. J. Wu, *J. Phys. Chem. B* **2005**, *109*, 13572.

[54] S. Yang, J. Gong, Y. Deng, *J. Mater. Chem.* **2012**, *22*, 13899.

[55] J. Huang, S. Virji, B. H. Weiller, R. B. Kaner, *J. Am. Chem. Soc.* **2003**, *125*, 314.

[56] Y. Yang, W. Guo, J. Qi, J. Zhao, Y. Zhang, *Appl. Phys. Lett.* **2010**, *97*, 223113.

[57] J. Zhou, Y. Gu, Y. Hu, W. Mai, P. H. Yeh, G. Bao, A. K. Sood, D. L. Polla, Z. L. Wang, *Appl. Phys. Lett.* **2009**, *94*, 191103.

[58] X. Chen, K. Liu, Z. Zhang, C. Wang, B. Li, H. Zhao, D. Zhao, D. Shen, *ACS Appl. Mater. Interfaces* **2016**, *8*, 4185.

[59] H. Endo, M. Kikuchi, M. Ashioi, Y. Kashiwaba, K. Hane, Y. Kashiwaba, *Appl. Phys. Express* **2008**, *1*, 051201.

[60] Q. Zheng, J. Huang, C. Han, Y. Chen, *IEEE Electron Device Lett.* **2017**, *38*, 79.

[61] M. Peng, Y. Liu, A. Yu, Y. Zhang, C. Liu, J. Liu, W. Wu, K. Zhang, X. Shi, J. Kou, *ACS Nano* **2015**, *10*, 1572.

[62] X. Sun, D. Li, Z. Li, H. Song, H. Jiang, Y. Chen, G. Miao, Z. Zhang, *Sci. Rep.* **2015**, *5*, 16819.

[63] H. Y. Chen, K. W. Liu, X. Chen, Z. Z. Zhang, M. M. Fan, M. M. Jiang, X. H. Xie, H. F. Zhao, D. Z. Shen, *J. Mater. Chem. C* **2014**, *2*, 9689.

[64] R. C. Wang, H. Y. Lin, C. H. Wang, C. P. Liu, *Adv. Funct. Mater.* **2012**, *22*, 3875.

[65] P. Lin, X. Yan, Z. Zhang, Y. Shen, Y. Zhao, Z. Bai, Y. Zhang, *ACS Appl. Mater. Interfaces* **2013**, *5*, 3671.

[66] S. Lu, J. Qi, S. Liu, Z. Zhang, Z. Wang, P. Lin, Q. Liao, Q. Liang, Y. Zhang, *ACS Appl. Mater. Interfaces* **2014**, *6*, 14116.

[67] L. Duan, F. He, Y. Tian, B. Sun, J. Fan, X. Yu, L. Ni, Y. Zhang, Y. Chen, W. Zhang, *ACS Appl. Mater. Interfaces* **2017**, *9*, 8161.